

---

# OPTIMAL DECISION MAKING IN HIGH-THROUGHPUT VIRTUAL SCREENING PIPELINES

---

**Hyun-Myung Woo**

Department of Electrical and Computer Engineering  
Texas A&M University  
College Station, TX 77843, USA  
larcwind@tamu.edu

**Xiaoning Qian**

Department of Electrical and Computer Engineering  
Texas A&M University  
College Station, TX 77843, USA  
xqian@ece.tamu.edu

**Li Tan**

Computational Science Initiative  
Brookhaven National Laboratory  
Upton, NY 11973, USA  
ltan@bnl.gov

**Shantenu Jha**

Computational Science Initiative  
Brookhaven National Laboratory  
Upton, NY 11973, USA  
shantenu@bnl.gov

**Francis J. Alexander**

Computational Science Initiative  
Brookhaven National Laboratory  
Upton, NY 11973, USA  
falexander@bnl.gov

**Edward R. Dougherty**

Department of Electrical and Computer Engineering  
Texas A&M University  
College Station, TX 77843, USA  
edward@ece.tamu.edu

**Byung-Jun Yoon**

Department of Electrical and Computer Engineering  
Texas A&M University  
College Station, TX 77843, USA  
bjyoon@ece.tamu.edu

September 27, 2021

## ABSTRACT

Effective selection of the potential candidates that meet certain conditions in a tremendously large search space has been one of the major concerns in many real-world applications. In addition to the nearly infinitely large search space, rigorous evaluation of a sample based on the reliable experimental or computational platform is often prohibitively expensive, making the screening problem more challenging. In such a case, constructing a high-throughput screening (HTS) pipeline that pre-sifts the samples expected to be potential candidates through the efficient earlier stages, results in a significant amount of savings in resources. However, to the best of our knowledge, despite many successful applications, no one has studied optimal pipeline design or optimal pipeline operations. In this study, we propose two optimization frameworks, applying to most (if not all) screening campaigns involving experimental or/and computational evaluations, for optimally determining the screening thresholds of an HTS pipeline. We validate the proposed frameworks on both analytic and practical scenarios. In particular, we consider the optimal computational campaign for the long non-coding RNA (lncRNA) classification as a practical example. To accomplish this, we built the high-throughput virtual screening (HTVS) pipeline for classifying the lncRNA. The simulation results demonstrate that the proposed frameworks significantly reduce the effective selection cost per potential candidate and make the HTS pipelines less sensitive to their structural variations. In addition to the validation, we provide insights on constructing a better HTS pipeline based on the simulation results.

**Keywords** Optimal computational campaign, optimal screening, optimal pipeline structure, optimization, high-throughput screening (HTS).

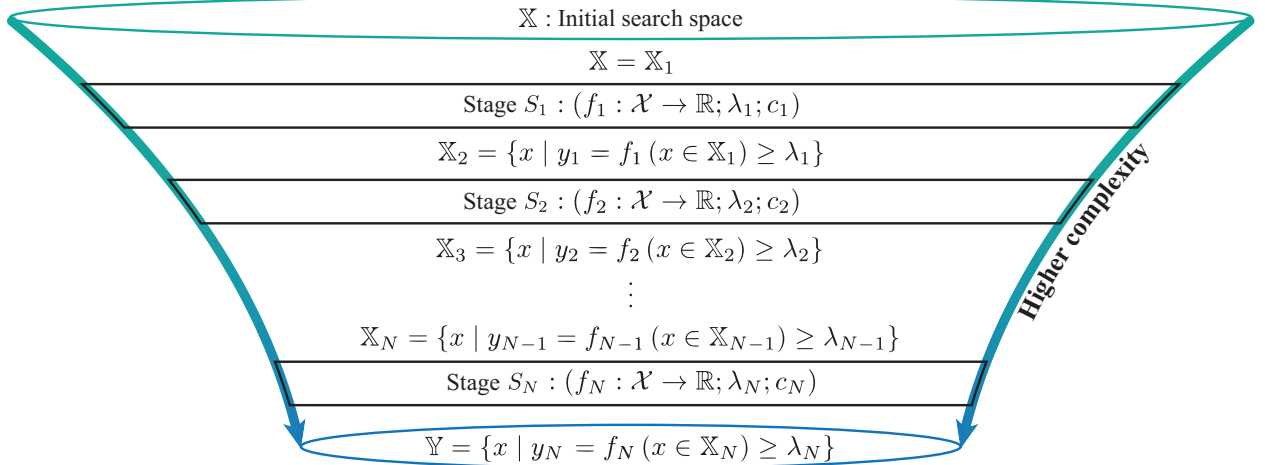


Figure 1: Illustration of the generalized high-throughput screening (HTS) pipeline with  $N$  stages for the rapid and reliable selection of a potential candidate set  $\mathbb{Y}$ . At each stage  $S_i$ , the evaluation platform  $f_i$  evaluates all the incoming samples  $x \in \mathbb{X}_i$  from the previous stage  $S_{i-1}$  and passes the samples whose score  $f_i(x)$  exceeds threshold  $\lambda_i$  to the next stage  $S_{i+1}$ .

## 1 Introduction

Effective selection of the potential candidates that meet certain conditions in a tremendously large search space has been one of the major concerns in many real-world applications. For example, amid the Coronavirus disease 2019 (COVID-19) pandemic [1], an urgent mission is finding molecules for developing a generally effective and side-effect-free vaccine. Besides, COVID-19 is rapidly evolving while mutating itself to survive against the vaccines in service [2]. As a result, the rapid selection of reliable potential molecules following the fast variations of the virus will become crucial to ending this pandemic.

In such a task, a fundamental challenge is, as we initially mentioned, to accurately yet efficiently sift the potential candidates satisfying certain conditions among infinitely many samples. In addition to the excessive numbers to evaluate, the experimental or computational cost of the evaluation for each candidate is often prohibitively expensive. To effectively explore such a nearly infinite space, a high-throughput screening (HTS) pipeline structure has been widely utilized in various fields across biology [3, 4, 5, 6, 7, 8], chemistry [9, 10, 11, 12, 13, 14, 15], engineering [16], and material science [17, 18]. In general, HTS pipelines consist of multiple stages, each of which is associated with either an experimental or computational platform that has different fidelity (*i.e.*, different accuracy and complexity) or is for filtering the samples from different perspectives from other platforms as shown in Fig. 1. A previous stage evaluates the samples through the associated an experimentally or computationally efficient platform and passes only the candidates whose score exceeds a certain threshold to the next stage associated with a experimentally or computationally expensive platform for a more sophisticated evaluation. In such a way, HTS can rapidly narrow down the search space and evaluate only the candidates that are highly likely to satisfy the golden criteria via the most sophisticated experimental or computational platform placed at the last stage. For example, in [7], a High-throughput virtual screening (HTVS) pipeline based on multi-fidelity computational algorithms combined with an experimental platform successfully selected and reported a novel-non-covalent inhibitor, MCULE-5948770040, that inhibits the SARS-Cov-2 main protease among over 6.5 million molecules. Besides, the HTS pipeline has been widely used for material selection. The first-principles high-throughput screening pipeline for non-linear optical materials (FHSP-NLO) [18] consists of several computational predictors, such as density functional theory code and data transformation and extraction code, followed by an experimental platform. FHSP-NLO successfully selected deep-ultraviolet non-linear optical crystals that were already reported in previous studies.

Although several studies have successfully demonstrated that constructing an HTS pipeline is indeed effective to narrow down and eventually sift the potential candidates in a nearly infinite search space, one ultimate question has not been properly addressed: What is the “optimal” HTS pipeline? In other words, how do we optimally determine the screening threshold of each stage for a given HTS structure? Beyond this question, can we improve the structure of the HTS pipeline? If so, what features of the evaluation platforms critically contribute to improving the performance of HTS pipeline? How many stages do we need? In what order should the platforms be placed?

In this study, we provide the answers to the questions. Specifically, we propose two general optimization frameworks that apply to any HTS pipeline campaigns whose primary objective is to effectively sift the potential candidates in an infinitely large search space. The first proposed framework estimates the optimal screening thresholds of the prior stages when there is a hard constraint on the total computational or experimental resource. The optimized pipeline is optimal in the sense that it maximally selects the potential candidates that pass the last stage with a hard budget constraint. The second optimization framework determines the optimal thresholds of the stages such that the optimized pipeline maximally identifies the potential candidates while minimizing the computational or experimental budget.

We validate the proposed optimization frameworks through two examples. We first attest to the efficacy of the proposed frameworks in the analytic scenario where the joint score distribution follows a multivariate Gaussian distribution. In the second example, we consider an optimal computational campaign for the long non-coding RNA (lncRNA) classification in keeping pace with the increasing interest of lncRNAs. lncRNA is a transcript longer than 200 nucleotides, which does not encode proteins. Several studies reported that the protein-coding RNAs account for less than 2% of the human genome, and up to 70% of non-coding genes are transcribed to lncRNAs [19, 20, 21]. In addition, researchers discovered that lncRNAs are closely related to Alzheimer’s diseases [22, 23, 24], cardiovascular diseases [25, 26], and several types of cancer development [27, 28, 29, 30]. Thus, a better understanding of the lncRNAs will pave the way forward to conquer such hard-to-treat diseases. In that regard, we build HTVS pipelines based on state-of-the-art lncRNA classification algorithms with various structures and evaluate the performance of the HTVS pipelines optimized through the proposed frameworks from various perspectives. Based on the simulation results, we provide insights into how one better constructs the HTS pipeline.

We organize the remaining sections as follows: In the next section, we mathematically describe the proposed optimization frameworks that find the optimal screening thresholds of the HTS pipeline. In Section 3, we comprehensively validate the proposed framework on two scenarios. Finally, we finish this work with some concluding remarks.

## 2 Methods

In this section, we propose the two optimization frameworks for optimizing an HTS pipeline for effective molecule selection: The first framework applies to the molecular selection campaign with a hard constraint on computational or experimental resources. The second framework considers the selection campaign without the hard resource constraint although it is desirable to minimize the resource. To develop the discussion, we first introduce a general setup for a molecular selection campaign within a fairly large search space.

Let us consider a general screening task identifying the potential candidate set  $\mathbb{Y} = \{x \mid f(x \in \mathbb{X}) \geq \lambda\}$  from a vast input set  $\mathbb{X}$ , where  $f : \mathcal{X} \rightarrow \mathbb{R}$  is a computational, experimental, or combined evaluation platform and  $\lambda$  is a screening threshold. We assume that  $\lambda$  is given by experts. In general, the evaluation cost per sample via  $f$  is prohibitively expensive, rendering the task infeasible. Let  $\mathcal{S}$  be a HTS pipeline for such a task consisting of  $N$  screening stages  $S_i : (f_i : \mathcal{X} \rightarrow \mathbb{R}; \lambda_i; c_i)$ ,  $i = 1, 2, \dots, N$ , connected in series as shown in Fig. 1, where  $f_i : \mathcal{X} \rightarrow \mathbb{R}$  is the evaluation platform,  $\lambda_i$  is a tunable screening threshold, and  $c_i$  is a computational or experimental cost per sample of the platform  $f_i$  associated with  $i$ th stage  $S_i$ , respectively. We assume that platform  $f_N$  of the last stage  $S_N$  is equivalent to  $f$  of the general screening task and screening threshold  $\lambda_N$  is given. Based on  $f_i$ , stage  $S_i$  evaluates the input samples  $x \in \mathbb{X}_i$ , at the cost of  $c_i$  per sample, that went through previous stage  $S_{i-1}$  and passes the samples of which the score  $y_i = f_i(x)$  exceeds threshold  $\lambda_i$  to the next stage  $S_{i+1}$ . Note that we do not consider dynamical process within the pipeline because the sampling process, especially for the first stage, critically affects the performance of the pipeline, which makes analysis complex. In other words, each stage collects all the input samples, evaluates them at the same time, and then passes them to the next stage. Formally, the output set  $\mathbb{X}_{i+1}$  of the stage  $S_i$ , which is an input set to the next stage  $S_{i+1}$ , is defined as follows:

$$\mathbb{X}_{i+1} = \{x \mid y_i = f_i(x \in \mathbb{X}_i) \geq \lambda_i\}, \quad (1)$$

where  $\mathbb{X}_i$  is the samples that passed  $S_{i-1}$ . Note that  $\mathbb{X}_{N+1} = \mathbb{Y}$ . In general, cost  $c_i$  is proportional to predictive accuracy. Hence, traditional HTS pipelines often have stages in series in the increasing order of  $c_i$ . Note that, for simplicity, we will use stage and platform in the same meaning.

A formal objective of the HTS pipeline is to determine the screening thresholds  $\lambda_i$  of the prior stages  $S_i$ ,  $i = 1, 2, \dots, N - 1$ , such that the HTS maximizes the cardinality of the potential candidate set  $\mathbb{Y}$  (i.e.,  $\max |\mathbb{Y}|$ ) with a limited resource budget  $C$  when the screening threshold  $\lambda_N$  of the last stage  $S_N$  is given. Under the assumption that the screening pipeline  $\mathcal{S}$  has been reasonably constructed, the scores of the samples  $\mathbb{X}$  across all the stages  $S_1, S_2, \dots, S_N$  are represented as a joint score distribution denoted as  $f_S(y_1, y_2, \dots, y_N)$ . Let us denote the

reward function  $r(\boldsymbol{\lambda})$  according to thresholds  $\boldsymbol{\lambda} = [\lambda_1, \lambda_2, \dots, \lambda_N]$  of the stages  $S_i, i = 1, 2, \dots, N$ , as follows:

$$r(\boldsymbol{\lambda}) = \int_{[\lambda_N, \lambda_{N-1}, \dots, \lambda_1]}^{\infty} \cdots \int_{\infty}^{\infty} f_S(y_1, y_2, \dots, y_N) dy_1 dy_2 \cdots dy_N. \quad (2)$$

Note that  $r(\boldsymbol{\lambda})$  is proportional to the number of the potential samples that went through the screening pipeline  $\mathcal{S}$ .

## 2.1 Optimization of a HTS pipeline under fixed computational budget

We first consider the case that there is a constraint on the computational or experimental budget  $C$ . As we described, we are interested in maximizing the number of potential candidates  $|\mathbb{Y}|$  passing the last screening stage  $S_N$  with computational budget  $C$ . We can find the optimal screening thresholds  $\boldsymbol{\psi}^* = [\lambda_1^*, \lambda_2^*, \dots, \lambda_{N-1}^*]$  of the prior stages  $S_i, i = 1, 2, \dots, N-1$ , maximizing  $|\mathbb{Y}|$ , by solving the constrained optimization problem as follows:

$$\boldsymbol{\psi}^* = \arg \max_{\boldsymbol{\psi} \in \mathbb{R}^{N-1}} r([\boldsymbol{\psi}, \lambda_N]) \quad (3)$$

$$\text{s.t.} \quad \sum_{i=1}^N c_i |\mathbb{X}_i| \leq C, \quad (4)$$

where  $|\mathbb{X}_i|$  is the number of samples that passed the previous stages from  $S_1$  to  $S_{i-1}$ , defined as follows:

$$|\mathbb{X}_i| = |\mathbb{X}| \int_{[\lambda_{i-1}, \lambda_{i-2}, \dots, \lambda_1]}^{\infty} \cdots \int_{\infty}^{\infty} f_{S_{1:i-1}}(y_1, y_2, \dots, y_{i-1}) dy_1 dy_2 \cdots dy_{i-1}. \quad (5)$$

## 2.2 Joint optimization of a HTS pipeline for efficiency and throughput

In critical real-world applications involving vaccine or drug development in urgent needs, the consideration of the throughput of the HTS pipeline is often prioritized before the resources. In addition, objectively considering different types of resources, such as time, human labor, money, difficulty, and computational resources, together is a more or less tricky task, affecting the overall performance of the HTS pipeline. In such a case, it will be desirable to “jointly” optimize the throughput of the pipeline and the resources as follows:

$$\boldsymbol{\psi}^* = \arg \min_{\boldsymbol{\psi} \in \mathbb{R}^{N-1}} \alpha g([\boldsymbol{\psi}, \lambda_N]) + (1 - \alpha) h([\boldsymbol{\psi}, \lambda_N]), \quad (6)$$

where  $\alpha \in [0, 1]$  is a weight parameter balancing between the relative reward function  $g([\boldsymbol{\psi}, \lambda_N])$  and the normalized total cost function  $h([\boldsymbol{\psi}, \lambda_N])$  defined respectively as follows:

$$g([\boldsymbol{\psi}, \lambda_N]) = \frac{r([-\infty, \lambda_N]) - r([\boldsymbol{\psi}, \lambda_N])}{r([-\infty, \lambda_N])} \quad (7)$$

$$= \frac{\int_{\lambda_N}^{\infty} f_{S_N}(y_N) dy_N - r([\boldsymbol{\psi}, \lambda_N])}{\int_{\lambda_N}^{\infty} f_{S_N}(y_N) dy_N}, \quad (8)$$

$$h([\boldsymbol{\psi}, \lambda_N]) = \frac{1}{N|\mathbb{X}| \max_i c_i} \sum_{i=1}^N c_i |\mathbb{X}_i|. \quad (9)$$

## 2.3 Learning the output relations across multiple stages in a HTS pipeline

Technically, the proposed optimization frameworks are two-phase approaches as they are dependent on the joint score distribution that needs to be estimated prior. In the first phase, we estimate the joint score distribution  $f_S(y_1, y_2, \dots, y_N)$ . Then, based on this, we estimate the optimal screening thresholds  $\lambda_i$  of the prior stages  $S_i, i = 1, 2, \dots, N-1$ . In this study, we consider the parametric spectral estimation under the assumption that the joint score distribution follows a multivariate Gaussian mixture model. If label information is available, we can find the parameters via maximum likelihood estimator (MLE) [31]. Otherwise, we can utilize the expectation-maximization (EM) algorithm [32].

### 3 Results

We validate the proposed frameworks in two scenarios. First, we study the analytic scenario where virtual score distribution  $f_S(y_1, y_2, \dots, y_N)$  follows a multivariate uni-modal Gaussian model. We assume that we have complete knowledge about the distribution  $f_S(y_1, y_2, \dots, y_N)$ . We analyze and compare the performance of the pipelines of the different structures optimized via the proposed frameworks with the baseline pipeline passing a certain proportion of the best samples to the next stages considered in [15, 33]. In this study, we assume the proportion is uniform across the stages (*i.e.*, the proportional values of the stages are identical). In the second scenario, we consider an optimal computational campaign for the lncRNA screening problem. To this aim, we construct various HTVS pipeline structures based on up to four existing state-of-the-art lncRNA classification algorithms. Then, we optimize the HTVS pipelines through the proposed frameworks. In this scenario, we assume that we have a small number of available samples (4% of total samples) to learn the joint score distribution  $f_S(y_1, y_2, y_3, y_4)$ . We compare the optimized pipelines with the last stage (*i.e.*,  $S_4$ ) and baseline pipelines from diverse perspectives. We optimize the objective function of each framework on both scenarios via the differential evolution optimizer [34] in the *Scipy Python* package (version 1.7.0). We performed all simulations on *Ubuntu* (version 20.04.2 LTS) installed on *Oracle VM VirtualBox* (version 6.1.22) that runs on a physical system equipped with *Intel i7-8809G* and 32 GB memory.

#### 3.1 Performance evaluation based on a synthetic HTS pipeline

Let us consider an analytic scenario in which we construct and optimize the HTS pipeline consisting of up to four stages (*i.e.*,  $N = 4$ ) of which the computational cost is 1, 10, 100, and 1000, respectively. The primary objective of the HTS pipeline is to maximize the number of potential candidates satisfying the given criterion (*i.e.*,  $f_4(x) \geq \lambda_4$ ) in the last stage  $S_4$  in an efficient manner. We assume that the number of initial samples is  $10^5$  and we have complete knowledge of the joint score distribution  $f_S(y_1, y_2, y_3, y_4)$  that follows a multivariate uni-modal Gaussian distribution  $\mathcal{G}(\mathbf{0}, \Sigma(\rho))$ , where the covariance matrix  $\Sigma(\rho)$  is a Toeplitz matrix defined as follows:

$$\Sigma(\rho) = \begin{bmatrix} 1 & \rho & \rho - 0.1 & \rho - 0.2 \\ \rho & 1 & \rho & \rho - 0.1 \\ \rho - 0.1 & \rho & 1 & \rho \\ \rho - 0.2 & \rho - 0.1 & \rho & 1 \end{bmatrix}, \quad (10)$$

where  $\rho \in [0, 1]$  is a maximum correlation between different stages. We assume that we are given  $\lambda_4 = 3.0902$  as prior information, resulting in 100 potential samples in initial sample set  $\mathbb{X}$ . We validate the proposed frameworks when  $\rho$  is 0.8 (high correlation) and 0.3 (low correlation). For the simulation results with various covariance matrices, see the supplementary information.

##### 3.1.1 Performance of the proposed HTS pipeline optimization method under fixed computational budget

Figure 2 shows the performance comparison results between the different HTS pipeline structures optimized via the proposed framework, discussed in Section 2.1, in terms of the number of the selected potential candidates to the total resource budget when  $\rho = 0.8$  (A. high correlation) and  $\rho = 0.3$  (B. low correlation), respectively. The black horizontal and vertical dashed lines stand for the number of true potential candidates (100 in this simulation) and the computational budget required when we screen the samples based on only the last stage  $S_4$ , respectively. Note that Fig. 2 shows only the performance of the best pipelines when  $N = 3$  and  $N = 4$ , respectively, and shows all the performance of the pipelines with two stages as references.

First, as shown in Fig. 2.A, the performance curves of the pipelines consisting of only two stages, marked as pink, purple, and light blue, respectively, demonstrate how each stage of different performance improves the performance of the pipeline on the proposed framework. To be specific, the degree of the correlation between a prior stage and the last stage determines the slope of the performance curve. In other words, the performance of the optimized pipeline with the most highly correlated prior stage  $S_3$ , marked in light blue, showed the steepest performance curve. On the other hand, the optimized pipeline with the least correlated prior stage  $S_1$ , marked in pink, showed the most gentle performance improvement as the total resource budget increases. However, the pipeline with the most computationally or experimentally efficient stage  $S_1$  was beneficial in the sense that it can evaluate all the samples fastest. In that regard, the pipeline with the slowest prior stage  $S_3$  was able to evaluate all the samples when all other optimized pipelines starting with either  $S_1$  or  $S_2$  selected more than 80% of the potential candidates. This simulation result demonstrates that constructing the pipeline with the efficient and accurate screening stage as the first stage is indeed effective when the resource budget is fairly limited.

Among the optimized pipelines with different structures, the pipeline with all the stages in the increasing order of correlation and complexity optimized through the proposed framework (*i.e.*,  $[S_1, S_2, S_3, S_4]$ , red solid line) consistently



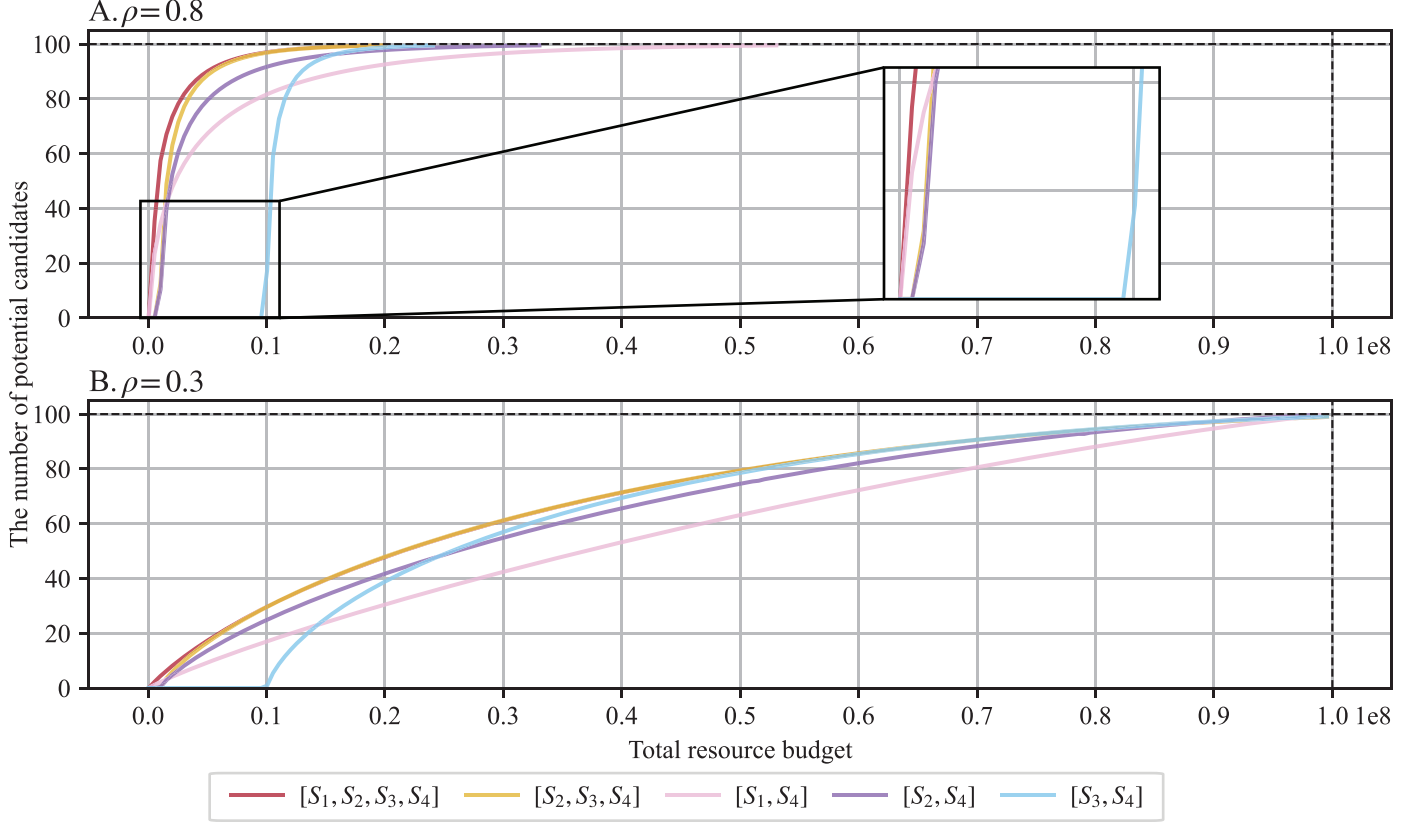


Figure 2: Comparison of the number of potential samples obtained via the pipelines optimized through the first proposed framework when the stages are either highly correlated (A,  $\rho = 0.8$ ) or less correlated (B,  $\rho = 0.3$ ). Note that only the best-performing configurations are shown for  $N \geq 3$ . For  $N = 2$ , all the pipelines are presented for comparison purposes. In general, the correlation between prior stages and the last stage determines the slope of the performance curve (the higher, the steeper), and the complexity of the first stage is closely related to the minimum budget for the complete evaluation of the samples.

showed the best performance while overcoming all the shortcomings that we have seen from two-stage pipelines. Specifically, the optimized pipeline  $[S_1, S_2, S_3, S_4]$  scanned all the samples through the most efficient stage  $S_1$  and based on the following stages that are more accurate improves the performance very sharply as the total resource increases. It selected 97% of the true potential candidates at 10% of the cost that requires evaluating all the samples through only the last stage (referred to as the original cost). To select 99% of the potential candidates, the optimized pipeline  $[S_1, S_2, S_3, S_4]$  needs only about 14% of the original cost. When the pipeline consists of three stages (*i.e.*,  $N = 3$ ), the optimized pipeline  $[S_2, S_3, S_4]$  showed the best performance among three-stage pipelines. As we analyzed, the performance sharply increased as the total amount of the resource increases due to the high correlation of the prior stages  $S_2$  and  $S_3$ . However, due to the less efficiency of the  $S_2$  compared to that of  $S_1$ , the performance started to jump relatively late compared to the optimized pipelines starting with  $S_1$ . In other words, the pipelines with three stages initially consumed more resources to evaluate all the samples through the  $S_2$ . Then, what will happen if we replace the  $S_2$  with  $S_1$ ? The simulation results (presented in the supplementary information) showed that pipelines  $[S_1, S_3, S_4]$  were able to initiate the selection of the potential candidate earlier but the slopes of the performance curves were more gentle compared to those of  $[S_2, S_3, S_4]$ . Considering all these points comprehensively, we could conclude that when all the prior stages have high correlations to the last stage, the best option is to place them in increasing order of the complexity and optimize them with the proposed framework.

Figure 2.B shows the performance comparison of the optimized pipelines when the correlation of the prior stages to the last stage is relatively low ( $\rho = 0.3$ ). Overall, the relative performance trend between the optimized pipelines is nearly identical to what we have seen in Fig. 2.A except that pipelines composed of low-correlation stages were significantly less efficient than pipelines composed of highly correlated stages. As we can see in Fig. 2.B when the available resource budget is about to reach the original cost, the optimized pipelines including the least efficient prior

Configuration	High correlation ( $\rho = 0.8$ )				Low correlation ( $\rho = 0.3$ )			
	Potential candidates	Total cost	Effective cost	Comp. savings	Potential candidates	Total cost	Effective cost	Comp. savings
$[S_4]$	100	100,000,000	1,000,000	0%	100	100,000,000	1,000,000	0%
$[S_1, S_4]$	94	22,372,654	238,007	76.20%	89	56,551,129	635,406	36.46%
$[S_2, S_4]$	96	15,511,702	161,580	83.84%	90	43,620,751	484,675	51.53%
$[S_3, S_4]$	98	18,152,330	185,228	81.48%	92	41,522,035	451,326	54.87%
$[S_1, S_2, S_4]$	97	17,890,176	184,435	81.56%	94	53,340,817	567,456	43.25%
$[S_1, S_3, S_4]$	98	14,451,644	147,466	85.25%	94	47,550,232	505,854	49.41%
$[S_2, S_1, S_4]$	97	18,291,054	188,568	81.14%	94	53,513,582	569,293	43.07%
$[S_2, S_3, S_4]$	98	13,089,779	133,569	86.64%	94	44,534,328	473,769	52.62%
$[S_3, S_1, S_4]$	99	19,505,326	197,023	80.30%	94	48,708,112	518,171	48.18%
$[S_3, S_2, S_4]$	99	19,522,312	197,195	80.28%	94	47,966,605	510,283	48.97%
$[S_1, S_2, S_3, S_4]$	99	14,147,264	142,902	85.71%	96	50,336,621	524,340	47.57%
$[S_1, S_3, S_2, S_4]$	99	15,939,108	161,001	83.90%	96	52,704,450	549,005	45.10%
$[S_2, S_1, S_3, S_4]$	99	14,348,794	144,937	85.51%	96	50,366,503	524,651	47.53%
$[S_2, S_3, S_1, S_4]$	99	14,335,230	144,800	85.52%	96	50,411,458	525,119	47.49%
$[S_3, S_1, S_2, S_4]$	99	20,560,571	207,682	79.23%	96	53,249,970	554,687	44.53%
$[S_3, S_2, S_1, S_4]$	99	20,560,299	207,680	79.23%	96	53,215,674	554,330	44.57%

Table 1: Performance comparison of various HTS pipeline structures jointly optimized via the proposed framework ( $\alpha = 0.5$ ) in terms of the number of potential candidates in the case that there is no constraint on budget.

approach	High correlation ( $\rho = 0.8$ )				Low correlation ( $\rho = 0.3$ )			
	Potential candidates	Total cost	Effective cost	Comp. savings	Potential candidates	Total cost	Effective cost	Comp. savings
Proposed	99	14,147,264	142,902	85.71%	96	50,336,621	524,340	47.57%
Baseline ( $R_s = 0.10$ )	26	400,000	15,385	98.46%	6	400,008	66,668	93.33%
Baseline ( $R_s = 0.25$ )	78	2,537,498	32,532	96.75%	28	2,537,516	90,626	90.94%
Baseline ( $R_s = 0.50$ )	98	15,599,934	159,183	84.08%	69	15,600,165	226,089	77.39%
Baseline ( $R_s = 0.75$ )	100	48,966,384	489,664	51.03%	93	48,662,387	523,251	47.67%

Table 2: Performance comparison of pipeline  $[S_1, S_2, S_3, S_4]$  configured via the proposed ( $\alpha = 0.5$ ) approach and baseline approach with different screening ratio  $R_s$  in terms of the number of potential samples in the case that there is no constraint on budget.

stage  $S_3$  were able to find 99% of the potential candidates with the original cost. However, considering that the average performance curve of  $[S_4]$  (i.e., without a pipeline structure) based on random sampling is a straight line connecting (0, 0) to the crossing point where the black horizontal and vertical lines meet, constructing pipelines was still effective with limited resources in an average sense. Based on the simulation results shown in Fig. 2.B, we could reach the same conclusion that the best pipeline structure is to place stages in order of increasing the complexity, and the proposed framework effectively optimizes the pipelines.

### 3.1.2 Performance of the proposed HTS pipeline optimization method for joint optimization of efficiency and throughput

Table 1 shows the performance of the various pipeline structures optimized via the joint optimization framework ( $\alpha = 0.5$ ) described in Section 2.2. Note that the second row (configuration  $[S_4]$ ) represents the performance of the last screening stage  $S_4$  without a pipeline as a reference. Effective cost is a ratio of the total cost to the number of potential candidates, standing for the average computational cost per potential candidate. The computational savings is calculated based on the effective cost. As we can see from Table 1, the second proposed optimization framework optimized the pipelines in a very robust manner to the change of the structure of the pipelines. The optimized pipelines consistently saved the resource from 76.20% to 86.64% of the original cost while selecting 94 ~ 99% of the true potential candidates when all the stages are highly correlated. Although the overall efficiency of the pipelines consisting of less correlated stages to the last stage ( $\rho = 0.3$ ) was less than the pipelines composed of highly correlated stages, the pipelines were indeed effective to save the resources. The optimized pipelines selected 89% 96% of the potential candidates at the effective cost of 531, 313 per sample on average.

For the comprehensive comparison of the optimized pipeline based on the proposed framework, we considered a baseline pipeline that simply passes the top  $R_s$  percentages of the samples to the next stage. Table 2 shows the performance comparison results when the pipeline consists of all the stages in the increasing order of the correlation and complexity (i.e.,  $[S_1, S_2, S_3, S_4]$ ). When the stages are highly correlated ( $\rho = 0.8$ ), the baseline pipelines with  $R_s = 0.1$  and 0.25 were more efficient than the optimized  $[S_1, S_2, S_3, S_4]$  based on the proposed framework. However, the baseline pipelines only selected 26% and 78% of the potential candidates, respectively. Considering that the primary goal of such a pipeline is to maximally select the potential candidates in an efficient manner, it did not achieve the goal properly. When  $R_s = 0.5$ , the baseline selected 98% of the true potential candidates at the effective cost of 159,183, which was worse performance compared to that of the optimized pipeline in terms of the selection capacity

Algorithm	Accuracy	Sensitivity	Specificity	Time per RNA (ms)
CPC2 [36]	0.7154	0.5760	0.9493	2.5265
CPAT [37]	0.8217	0.6861	0.9817	2.7336
PLEK [38]	0.7050	0.5666	0.9478	83.1765
LncFinder [39]	0.8329	0.7062	0.9678	2,495.6231

Table 3: Performance comparison of the stages that make up the HTS pipeline for identification of the lncRNA.



Figure 3: One of the optimal structures of the HTVS pipeline for selecting lncRNAs.

and the efficiency. When  $R_s = 0.75$ , the efficiency of the baseline pipeline significantly dropped to 51.03% to select 100% of the samples. Note that, different from the proposed frameworks, the baseline approach does not involve the joint score estimation process. In other words, we can not determine the optimal  $R_s$  prior, which degrades the performance of the baseline pipeline significantly in practice. When the correlation between the stages is relatively low ( $\rho = 0.3$ ), all the baselines were unable to select the potential candidates as many as the optimized pipeline selected. Considering all the results shown in Tables 1 and 2, the proposed optimization framework discussed in Section 2.2 ( $\alpha = 0.5$ ) indeed effectively optimizes the pipelines such that the optimized pipelines are able to select most of the true potential candidates with reasonable resource consumption.

### 3.2 Building an optimal high-throughput virtual screening pipeline for detecting lncRNAs

To demonstrate the efficacy of the proposed optimization frameworks, we considered an optimal computational campaign for the identification of the lncRNAs among transcripts. As we described in the introduction, there have been explosively increasing interests in the roles of lncRNAs in biological processes as several studies reported that lncRNAs are closely related to the development of hard-to-treat diseases including Alzheimer’s diseases [22, 23, 24], cardiovascular diseases [25, 26], and several types of cancers [27, 28, 29, 30]. In that regard, accurate identification of the lncRNAs is a fundamental and critical step in disease treatment studies. To this aim, we constructed an HTVS pipeline for identifying lncRNA based on the existing computational algorithms and applied the proposed optimization frameworks to the HTVS to find the optimal screening thresholds of stages.

#### 3.2.1 Dataset

We collected nucleotide sequences of RNA transcripts on the human reference chromosomes, consisting of 48,752 lncRNA sequences and 106,143 protein-coding sequences, from GENCODE v38 (May 5, 2021). We filtered out the sequences containing invalid characters other than A, U, C, or G and the sequences of which the length exceeds 3,000nt, resulting in 45,216 lncRNA sequences 79,030 protein-coding sequences. Lastly, we applied a clustering algorithm CD-hit [35] to lncRNAs and protein-coding RNAs, respectively, to remove redundant sequences. As a result, We have 104,733 RNA sequences consisting of 39,785 lncRNA and 64,948 protein-coding sequences.

#### 3.2.2 Construction of the lncRNA HTVS pipeline

As seen in the simulation results on the analytic scenario, the efficacy of the HTS pipeline is critically dependent on the correlation between the prior stages and the golden-standard stage (*i.e.*, the last stage). In that regard, we selected four state-of-the-art computational algorithms, which have been widely used and highly cited, estimating the coding potential probability: CPC2 [36], CPAT [37], PLEK [38], and LncFinder [39].

To better understand the algorithms, we first evaluated the performance of the algorithms on the pre-processed dataset as shown in Table 3. Note that we computed the accuracy, sensitivity, and specificity of the results based on hard-decision values (*i.e.*, either 0 or 1) estimated by the algorithms. For those that do not output the hard-decision value, we set 0.5 to the decision boundary. As shown in Table 3, LncFinder showed the accuracy, sensitivity, and specificity of 0.8329, 0.7062, and 0.9678, respectively, outperforming all the algorithms in terms of accuracy and sensitivity at the cost of the highest computational complexity (2,495.6231 milliseconds per sample). CPAT was the second-best performer in terms of accuracy and sensitivity and recorded the best specificity. CPC2 and PLEK were the third and worst performers, respectively, in terms of accuracy, sensitivity, and specificity. CPC2 and CPAT were not only computationally efficient but also highly accurate compared to the worst performer PLEK. Based on the evaluation



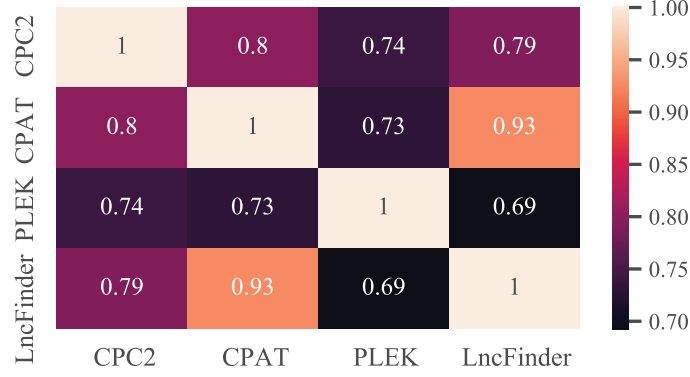


Figure 4: The Heat map of Pearson’s correlation coefficient between stages. CPAT is highly correlated to the golden standard filter LncFinder.

result, we set the LncFinder as the final stage and constructed a basic HTVS pipeline structure as shown in Fig. 3. Next, we computed Pearson’s correlation coefficient between scores estimated by the algorithms. As shown in Fig. 4, CPAT showed 0.93 of the correlation coefficient to the LncFinder, yielding the highest correlation among the prior algorithms.

We estimated the joint score distribution  $f_S(y_1, y_2, y_3, y_4)$  via the EM algorithm with 4% of the samples. Note that the computational lncRNA identification algorithms used in this study output protein-coding probability, meaning that a higher value corresponds to the higher chance to be a protein-coding sequence. Since our goal is to identify the lncRNAs, we multiplied the output of the algorithms by  $-1$  such that the higher values represent a higher chance to be the lncRNA. In addition, we assumed that  $\lambda_4 = 0.2$  as prior information.

### 3.2.3 Optimizing lncRNA screening performance under computational budget constraint

Figure 5 shows the performance comparison results of the optimized HTVS pipelines with various structures. The black horizontal and vertical dashed lines represent the number of true potential candidates and the computational cost for the complete evaluation of all the samples based on the last stage LncFinder, respectively. Black vertical dotted lines are located at intervals of 1/10 of the original cost. Underneath each dotted line, the number of potential candidates selected by each optimized pipeline is summarized. As we have seen in the analytic scenario, the complexity of the initial stage in the pipeline determined the point where the pipeline starts to select the potential candidates, and the correlation between a stage and the last stage was closely related to the slope of the performance curve. For example, when the optimized pipelines consume 10% of the original cost, the pipelines starting with the third stage (*i.e.*, PLEK) showed the worst performance in terms of the selection capability. Specifically,  $[S_3, S_4]$ ,  $[S_3, S_1, S_4]$ ,  $[S_3, S_2, S_4]$ ,  $[S_3, S_1, S_2, S_4]$ , and  $[S_3, S_2, S_1, S_4]$  found the potential candidates of 6, 218, 6, 530, 6, 607, 6, 448, and 6, 601, respectively. The other optimized pipelines starting with either  $S_1$  or  $S_2$  (*i.e.*, CPC2 or CPAT) selected the potential candidates from 9, 518 to 10, 033. In addition, the pipeline including the second stage associated with CPAT that is highly correlated to the last stage showed the steepest slope of the performance curves. As a result, all the optimized pipelines including CPAT, regardless of the order of the stages, identified from 45, 697 to 47, 466 of the potential candidates at only 50% of the original cost. Interestingly, the proposed framework was effective to robustly configure the pipeline such that it consistently performs well even in the presence of the stage that is computationally complex but less correlated to the last stage. Specifically, although the optimized pipeline  $[S_1, S_2, S_4]$  outperformed the optimized pipeline  $[S_1, S_2, S_3, S_4]$ , the performance gap was relatively small. The maximum difference in the number of selected potential candidates was 1, 202 when the pipelines consumed 40% of the original cost. However, considering the much heavier computational complexity and the less correlation of the third stage, the performance difference is nearly negligible as 1, 202 is only about 2.4% of the true potential candidates. In addition, the difference was drastically reduced as the available computational resources increase and there was only a difference of 50 between the pipelines when they consumed 70% of the original cost. In practice, HTS or HTVS pipelines can include various types of platforms, some of which may not be closely correlated to the last stage to screen samples from completely different perspectives. In such a case, it is important to optimize the pipelines such that it consistently performs well even in presence of such less correlated stages.

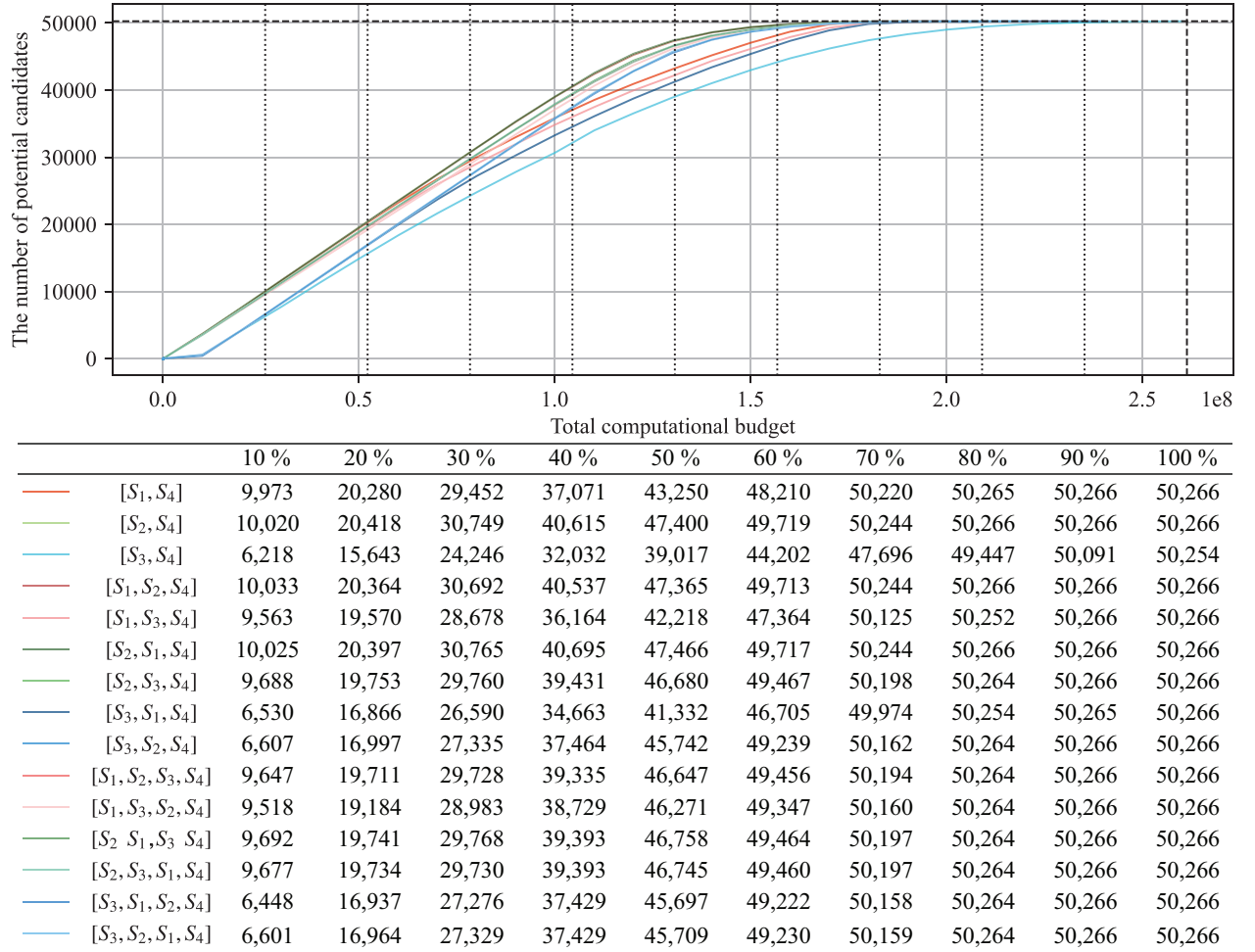


Figure 5: Performance comparison of the HTS pipelines, designed for identifying the lncRNAs and optimized via the proposed approach, in terms of the number of potential samples in the case that there is a hard constraint on the computational budget ( $x$ -axis). The performance of the pipelines optimized via the proposed framework was not significantly affected by their structure.

Configuration	Potential candidates	Total cost (ms)	Effective cost	Computational savings	Accuracy	Sensitivity	Specificity	F1
[S <sub>4</sub> ]	50,266	261,374,090	5,200	0%	0.8440	0.9264	0.7936	0.8186
[S <sub>1</sub> , S <sub>4</sub> ]	48,875	161,357,081	3,301	36.52%	0.8429	0.9075	0.8034	0.8144
[S <sub>2</sub> , S <sub>4</sub> ]	47,950	134,366,143	2,802	46.12%	0.8624	0.9215	0.8262	0.8357
[S <sub>3</sub> , S <sub>4</sub> ]	47,083	176,963,736	3,758	27.73%	0.8450	0.8876	0.8188	0.8131
[S <sub>1</sub> , S <sub>2</sub> , S <sub>4</sub> ]	48,210	134,748,992	2,795	46.25%	0.8600	0.9216	0.8222	0.8333
[S <sub>1</sub> , S <sub>3</sub> , S <sub>4</sub> ]	49,100	168,490,516	3,432	34.00%	0.8442	0.9120	0.8026	0.8164
[S <sub>2</sub> , S <sub>1</sub> , S <sub>4</sub> ]	48,214	134,812,024	2,796	46.23%	0.8600	0.9216	0.8222	0.8334
[S <sub>2</sub> , S <sub>3</sub> , S <sub>4</sub> ]	48,295	141,710,246	2,934	43.58%	0.8602	0.9230	0.8218	0.8338
[S <sub>3</sub> , S <sub>1</sub> , S <sub>4</sub> ]	49,119	171,803,403	3,498	32.73%	0.8444	0.9124	0.8026	0.8166
[S <sub>3</sub> , S <sub>2</sub> , S <sub>4</sub> ]	48,326	146,100,080	3,023	41.86%	0.8600	0.9231	0.8214	0.8336
[S <sub>1</sub> , S <sub>2</sub> , S <sub>3</sub> , S <sub>4</sub> ]	48,402	140,954,256	2,912	44.00%	0.8591	0.9228	0.8200	0.8326
[S <sub>1</sub> , S <sub>3</sub> , S <sub>2</sub> , S <sub>4</sub> ]	48,332	141,229,518	2,922	43.81%	0.8587	0.9215	0.8203	0.8321
[S <sub>2</sub> , S <sub>1</sub> , S <sub>3</sub> , S <sub>4</sub> ]	48,409	141,022,859	2,913	43.98%	0.8591	0.9229	0.8200	0.8326
[S <sub>2</sub> , S <sub>3</sub> , S <sub>1</sub> , S <sub>4</sub> ]	48,414	141,225,328	2,917	43.90%	0.8591	0.9230	0.8200	0.8327
[S <sub>3</sub> , S <sub>1</sub> , S <sub>2</sub> , S <sub>4</sub> ]	48,424	145,321,388	3,001	42.29%	0.8589	0.9228	0.8197	0.8324
[S <sub>3</sub> , S <sub>2</sub> , S <sub>1</sub> , S <sub>4</sub> ]	48,429	145,388,626	3,002	42.27%	0.8589	0.9229	0.8197	0.8325

Table 4: Performance evaluation of HTVS pipelines with various structures. Each pipeline was optimized via the proposed optimization framework with the balancing weight  $\alpha = 0.5$ .

Approach	Potential candidates	Total cost (ms)	Effective cost	Computational savings	Accuracy	Sensitivity	Specificity	F1
Proposed	48,402	140,954,256	2,912	44.00%	0.8591	0.9228	0.8200	0.8326
Baseline ( $R_s = 0.25$ )	1,402	4,963,415	3,540	31.92%	0.6318	0.0330	0.9986	0.0638
Baseline ( $R_s = 0.5$ )	12,653	35,255,772	2,786	46.42%	0.7170	0.2866	0.9807	0.4348
Baseline ( $R_s = 0.75$ )	39,079	115,643,459	2,959	43.10%	0.8366	0.7761	0.8737	0.7801

Table 5: Performance comparison of pipeline  $[S_1, S_2, S_3, S_4]$  jointly optimized via the proposed platform ( $\alpha = 0.5$ ) or set up through the baseline approach with a different screening ratio  $R_s$ .

### 3.2.4 Joint optimization of the lncRNA HTS pipeline for efficiency and accuracy

We validated the performance of the pipelines jointly optimized through the proposed framework ( $\alpha = 0.5$ ) described in Section 2.2 when there is no budget constraint as shown in Table 4. On average, the optimized pipelines selected 48,372 potential candidates out of 50,266 true potential candidates throughout the simulation at the effective cost of 3,067. As we expected, optimized pipelines including the second stage  $S_2$  associated with CPAT achieved relatively high computational savings (from 41.86% to 46.25%) compared to those without  $S_2$  (from 27.73% to 36.52%). As similar to what we have observed in the analytic scenario, the optimization frame was indeed effective to reduce the performance degradation caused by the presence of the stage associated with a less correlated and computationally complex algorithm (*i.e.*, PLEK). In other words, the selection capability of the pipeline optimized via the proposed framework was mainly dependent on the best-performing prior stage in the pipeline. Furthermore, the proposed framework significantly reduced the performance dependency on the order of the stages within the pipeline. For example, when one utilizes all the stages ( $N = 4$ ), the optimized pipelines selected 48,402 potential candidates on average and consistently saved the computational resources from 42.27% to 44.00%. We also evaluated the quality of the potential candidates selected by the HTS pipelines in terms of accuracy, sensitivity, specificity, and F1 score. Interestingly, all the optimized pipelines except for  $[S_1, S_4]$  outperformed LncFinder in terms of accuracy. In terms of sensitivity, the optimized pipeline achieved 0.9177. All the pipelines achieved higher specificity compared to LncFinder. Besides, the optimized pipelines including  $S_2$  consistently outperformed LncFinder in terms of the F1 score.

Finally, we compared the performance of the optimized pipeline with that of the baseline approach passing a fixed proportion of incoming samples to the next stage as shown in Table 5. Overall, all the baseline pipelines selected fewer potential candidates than what the optimized pipeline found. When  $R_s = 0.25$ , meaning the top 25% of incoming samples passed to the next stage, only selected 1,402 potential candidates with less computational savings (31.92%) compared to the optimized pipeline. Although the baseline with  $R_s = 0.5$  achieved slightly higher computational savings (46.42%) compared to that of the optimized pipeline (44.00%), the selection capability of the baseline pipeline was significantly worse than the optimized pipeline. Even we increased  $R_s$  to 0.75, the baseline still selected only 39,079 potential candidates with slightly worse computational savings. Besides, in terms of the quality of the potential candidates, except for the specificity, the optimized pipelines outperformed the baselines in terms of all other metrics. Note that the reason for the higher specificity of the baseline pipeline is due to much less number of the selected potential candidates.

## 4 Concluding Remarks

In this work, we proposed two optimization frameworks estimating the optimal screening thresholds of the high-throughput screening (HTS) pipeline. The first framework applies to screening tasks where there is a constraint on resource budget, and the second framework works for screening tasks with no limitations on budgets. We validated the frameworks on both analytic and practical scenarios. In analytic simulation results showed the optimized pipelines consistently achieved better performance compared to the baseline. In addition, the performance of the optimized pipelines was less sensitive to the order of the stages if it includes at least one highly correlated prior stage to the last stage. In other words, the performance of the optimized pipeline was mainly dependent on the most highly related stage rather than the order of the stages. Considering that in real-world applications, HTS pipelines often install less correlated stages on purpose to filter out the samples from different perspectives, the optimization frameworks were highly effective to reduce the such a problem that the traditional pipelines suffered from. Indeed, we validated such a case through the computational campaign for selecting the lncRNAs. The pipeline including highly accurate and efficient stages (CPC2 and CPAT) showed the best performance regardless of the order of the stages. Besides, the optimized pipeline including CPAT effectively reduced the performance degradation caused by the presence of the less correlated but computationally complex stage (PLEK).

In addition to demonstration of the efficacy of the frameworks, based on the comprehensive simulation results, we provided insights on how to better construct the HTS pipeline on the optimized frameworks: First, to achieve better

performance, it is essential to install an efficient stage closely related to the last stage in the HTS pipeline. Second, one of the reliable strategies to place the stages in the HTS pipeline is to place them in the increasing order of the complexity as it allows the pipeline to take a quick initial evaluation. Third, inefficient and less correlated stages can significantly decrease the performance of HTS pipelines, therefore it is highly recommended to minimize their use or, at least, to utilize them together with a highly related and efficient stage as the performance of the optimized pipeline is mainly dependent on the best performing stages.

Finally, we emphasize that the proposed optimization frameworks apply to a wide range of HTS pipelines involved in various real-world applications as they are designed based on fairly general assumptions. As we discussed previously, amid the COVID-19 pandemic, there has been an explosive need for the immediate selection of promising candidate molecules for the COVID-19 vaccine. In that regard, applying the proposed frameworks to a pipeline for potential candidate selection for the COVID-19 vaccine, possibly consisting of experimental and computational stages, will be an interesting future direction. In such a case, accurate estimation of the joint score distribution is one of the key issues. In that regard, it may be helpful to introduce the Bayesian framework. Specifically, one can build a prior distribution based on the domain knowledge we have accumulated and repeatedly update the posterior distribution based on evaluation results of the samples through the stages.

## References

- [1] I. Chakraborty and P. Maity, "Covid-19 outbreak: Migration, effects on society, global environment and prevention," *Science of the Total Environment*, vol. 728, p. 138882, 2020.
- [2] B. Roy, J. Dhillon, N. Habib, and B. Pugazhandhi, "Global variants of covid-19: Current understanding," *Journal of Biomedical Sciences*, vol. 8, no. 1, pp. 8–11, 2021.
- [3] N. Rieber, B. Knapp, R. Eils, and L. Kaderali, "Rnaither, an automated pipeline for the statistical analysis of high-throughput rna screens," *Bioinformatics*, vol. 25, no. 5, pp. 678–679, 2009.
- [4] M. H. Studer, J. D. DeMartini, S. Brethauer, H. L. McKenzie, and C. E. Wyman, "Engineering of a high-throughput screening system to identify cellulosic biomass, pretreatments, and enzyme formulations that enhance sugar release," *Biotechnology and Bioengineering*, vol. 105, no. 2, pp. 231–238, 2010.
- [5] A. Hartmann, T. Czauderna, R. Hoffmann, N. Stein, and F. Schreiber, "Htpheno: an image analysis pipeline for high-throughput plant phenotyping," *BMC bioinformatics*, vol. 12, no. 1, pp. 1–9, 2011.
- [6] K. Sikorski, A. Mehta, M. Inngjerdigen, F. Thakor, S. Kling, T. Kalina, T. A. Nyman, M. E. Stensland, W. Zhou, G. A. de Souza, *et al.*, "A high-throughput pipeline for validation of antibodies," *Nature methods*, vol. 15, no. 11, pp. 909–912, 2018.
- [7] A. Clyde, S. Galanie, D. W. Kneller, H. Ma, Y. Babuji, B. Blaiszik, A. Brace, T. Brettin, K. Chard, R. Chard, *et al.*, "High throughput virtual screening and validation of a sars-cov-2 main protease non-covalent inhibitor," *bioRxiv*, 2021.
- [8] A. Clyde, T. Brettin, A. Partin, H. Yoo, Y. Babuji, B. Blaiszik, A. Merzky, M. Turilli, S. Jha, A. Ramanathan, *et al.*, "Protein-ligand docking surrogate models: A sars-cov-2 benchmark for deep learning accelerated virtual screening," *arXiv preprint arXiv:2106.07036*, 2021.
- [9] R. L. Martin, C. M. Simon, B. Smit, and M. Haranczyk, "In silico design of porous polymer networks: high-throughput screening for methane storage materials," *Journal of the American Chemical Society*, vol. 136, no. 13, pp. 5006–5022, 2014.
- [10] L. Cheng, R. S. Assary, X. Qu, A. Jain, S. P. Ong, N. N. Rajput, K. Persson, and L. A. Curtiss, "Accelerating electrolyte discovery for energy storage with high-throughput screening," *The journal of physical chemistry letters*, vol. 6, no. 2, pp. 283–291, 2015.
- [11] J. J. F. Chen and D. P. Visco Jr, "Developing an in silico pipeline for faster drug candidate discovery: Virtual high throughput screening with the signature molecular descriptor using support vector machine models," *Chemical Engineering Science*, vol. 159, pp. 31–42, 2017.
- [12] D. L. Filer, P. Kothiya, R. W. Setzer, R. S. Judson, and M. T. Martin, "tcpl: the toxcast pipeline for high-throughput screening data," *Bioinformatics*, vol. 33, no. 4, pp. 618–620, 2017.
- [13] Y. Li, J. Zhang, N. Wang, H. Li, Y. Shi, G. Guo, K. Liu, H. Zeng, and Q. Zou, "Therapeutic drugs targeting 2019-ncov main protease by high-throughput screening," *BioRxiv*, 2020.
- [14] R. T. Rebbeck, D. P. Singh, K. A. Janicek, D. M. Bers, D. D. Thomas, B. S. Launikonis, and R. L. Cornea, "Ryr1-targeted drug discovery pipeline integrating fret-based high-throughput screening and human myofiber dynamic ca 2+ assays," *Scientific reports*, vol. 10, no. 1, pp. 1–13, 2020.

- [15] A. A. Saadi, D. Alfe, Y. Babuji, A. Bhati, B. Blaiszik, T. Brettin, K. Chard, R. Chard, P. Coveney, A. Tri-fan, *et al.*, “Impeccable: Integrated modeling pipeline for covid cure by assessing better leads,” *arXiv preprint arXiv:2010.06574*, 2020.
- [16] A. Tran, T. Wildey, and S. McCann, “smf-bo-2cogp: A sequential multi-fidelity constrained bayesian optimization framework for design applications,” *Journal of Computing and Information Science in Engineering*, vol. 20, no. 3, 2020.
- [17] Q. Yan, J. Yu, S. K. Suram, L. Zhou, A. Shinde, P. F. Newhouse, W. Chen, G. Li, K. A. Persson, J. M. Gre-goire, *et al.*, “Solar fuels photoanode materials discovery by integrating high-throughput theory and experiment,” *Proceedings of the National Academy of Sciences*, vol. 114, no. 12, pp. 3040–3043, 2017.
- [18] B. Zhang, X. Zhang, J. Yu, Y. Wang, K. Wu, and M.-H. Lee, “First-principles high-throughput screening pipeline for nonlinear optical materials: Application to borates,” *Chemistry of Materials*, vol. 32, no. 15, pp. 6772–6779, 2020.
- [19] S. Djebali, C. A. Davis, A. Merkel, A. Dobin, T. Lassmann, A. Mortazavi, A. Tanzer, J. Lagarde, W. Lin, F. Schlesinger, *et al.*, “Landscape of transcription in human cells,” *Nature*, vol. 489, no. 7414, pp. 101–108, 2012.
- [20] E. Pennisi, “Encode project writes eulogy for junk dna,” 2012.
- [21] Q. Yang, S. Zhang, H. Liu, J. Wu, E. Xu, B. Peng, and Y. Jiang, “Oncogenic role of long noncoding rna af118081 in anti-benzo [a] pyrene-trans-7, 8-dihydrodiol-9, 10-epoxide-transformed 16hbe cells,” *Toxicology letters*, vol. 229, no. 3, pp. 430–439, 2014.
- [22] S.-Y. Ng, L. Lin, B. S. Soh, and L. W. Stanton, “Long noncoding rnas in development and disease of the central nervous system,” *Trends in Genetics*, vol. 29, no. 8, pp. 461–468, 2013.
- [23] L. Tan, J.-T. Yu, N. Hu, and L. Tan, “Non-coding rnas in alzheimer’s disease,” *Molecular neurobiology*, vol. 47, no. 1, pp. 382–393, 2013.
- [24] Q. Luo and Y. Chen, “Long noncoding rnas and alzheimer’s disease,” *Clinical interventions in aging*, vol. 11, p. 867, 2016.
- [25] A. Congrains, K. Kamide, R. Oguro, O. Yasuda, K. Miyata, E. Yamamoto, T. Kawai, H. Kusunoki, H. Yamamoto, Y. Takeya, *et al.*, “Genetic variants at the 9p21 locus contribute to atherosclerosis through modulation of anril and cdkn2a/b,” *Atherosclerosis*, vol. 220, no. 2, pp. 449–455, 2012.
- [26] Z. Xue, S. Hennelly, B. Doyle, A. A. Gulati, I. V. Novikova, K. Y. Sanbonmatsu, and L. A. Boyer, “A g-rich motif in the lncrna braveheart interacts with a zinc-finger transcription factor to specify the cardiovascular lineage,” *Molecular cell*, vol. 64, no. 1, pp. 37–50, 2016.
- [27] G. Yang, X. Lu, and L. Yuan, “Lncrna: a link between rna and cancer,” *Biochimica et Biophysica Acta (BBA)-Gene Regulatory Mechanisms*, vol. 1839, no. 11, pp. 1097–1109, 2014.
- [28] X. Shi, M. Sun, H. Liu, Y. Yao, R. Kong, F. Chen, and Y. Song, “A critical role for the long non-coding rna gas5 in proliferation and apoptosis in non-small-cell lung cancer,” *Molecular carcinogenesis*, vol. 54, no. S1, pp. E1–E12, 2015.
- [29] W.-X. Peng, P. Koirala, and Y.-Y. Mo, “Lncrna-mediated regulation of cell signaling in cancer,” *Oncogene*, vol. 36, no. 41, pp. 5661–5667, 2017.
- [30] J. Carlevaro-Fita, A. Lanzós, L. Feuerbach, C. Hong, D. Mas-Ponte, J. S. Pedersen, and R. Johnson, “Cancer lncrna census reveals evidence for deep functional conservation of long noncoding rnas in tumorigenesis,” *Communications biology*, vol. 3, no. 1, pp. 1–16, 2020.
- [31] C. M. Bishop, “Pattern recognition,” *Machine learning*, vol. 128, no. 9, 2006.
- [32] A. P. Dempster, N. M. Laird, and D. B. Rubin, “Maximum likelihood from incomplete data via the em algorithm,” *Journal of the Royal Statistical Society: Series B (Methodological)*, vol. 39, no. 1, pp. 1–22, 1977.
- [33] M. U. Mirza and M. Froeyen, “Structural elucidation of sars-cov-2 vital proteins: Computational methods reveal potential drug candidates against main protease, nsp12 polymerase and nsp13 helicase,” *Journal of pharmaceutical analysis*, vol. 10, no. 4, pp. 320–328, 2020.
- [34] R. Storn and K. Price, “Differential evolution—a simple and efficient heuristic for global optimization over continuous spaces,” *Journal of global optimization*, vol. 11, no. 4, pp. 341–359, 1997.
- [35] W. Li and A. Godzik, “Cd-hit: a fast program for clustering and comparing large sets of protein or nucleotide sequences,” *Bioinformatics*, vol. 22, no. 13, pp. 1658–1659, 2006.



- [36] Y.-J. Kang, D.-C. Yang, L. Kong, M. Hou, Y.-Q. Meng, L. Wei, and G. Gao, "Cpc2: a fast and accurate coding potential calculator based on sequence intrinsic features," *Nucleic acids research*, vol. 45, no. W1, pp. W12–W16, 2017.
- [37] L. Wang, H. J. Park, S. Dasari, S. Wang, J.-P. Kocher, and W. Li, "Cpat: Coding-potential assessment tool using an alignment-free logistic regression model," *Nucleic acids research*, vol. 41, no. 6, pp. e74–e74, 2013.
- [38] A. Li, J. Zhang, and Z. Zhou, "Plek: a tool for predicting long non-coding rnas and messenger rnas based on an improved k-mer scheme," *BMC bioinformatics*, vol. 15, no. 1, pp. 1–10, 2014.
- [39] S. Han, Y. Liang, Q. Ma, Y. Xu, Y. Zhang, W. Du, C. Wang, and Y. Li, "Lncfinder: an integrated platform for long non-coding rna identification utilizing sequence intrinsic composition, structural information and physico-chemical property," *Briefings in bioinformatics*, vol. 20, no. 6, pp. 2009–2027, 2019.